Research Article

Muslim Abdul-Ameer Al-Kannoon* and Hayder Wafi Al-Thabhawee

Cyclic performance of moment connections with reduced beam sections using different cut-flange profiles

https://doi.org/10.1515/eng-2022-0354 received April 10, 2022; accepted July 05, 2022

Abstract: Reduced beam section (RBS) behaviours with various cut-flange configurations were investigated numerically in this study. A three-dimensional finite element model material non-linearity was built and validated experimentally, and the impacts of the cut-flange profile on the moment-rotation behaviour and ductility response of moment-resisting connections were investigated in a parametric form. Five-moment connections with various forms of decreasing beam flange were thus modelled using ABAQUS software and compared in terms of cyclic behaviour. RBS with circular, rectangular, trapezoidal, triangular, and drilled holes cut-flange configurations were adopted, and the finite element analysis results showed that radius cut RBS have uniform stress contours, while a reentrant corner in rectangular, trapezoidal, or triangular cutflange profiles' connections may result in stress concentration, resulting in a fracture of the flange. In addition, the numerical testing showed that the RBS connection with a circular cutflange profile offers a lower rupture index than other connections. Thus, the RBS created using circular cut-flange profiles dissipates more energy than other connections.

Keywords: cyclic loading, ductility response, moment-rotation response, reduced beam section

1 Introduction

Over recent decades, earthquakes have revealed several vulnerabilities in various steel moment-resisting frames.

* Corresponding author: Muslim Abdul-Ameer Al-Kannoon,
Department of Civil Engineering, Faculty of Engineering, Kufa University,
Al-Najaf City, Iraq, e-mail: muslim.altameemi@uokufa.edu.iq
Hayder Wafi Al-Thabhawee: Department of Civil Engineering,
Faculty of Engineering, Kufa University, Al-Najaf City, Iraq,
e-mail: hayder.althabhawi@uokufa.edu.iq

Within seismically active zones, steel frame construction had previously increased because it was thought to be sufficiently ductile for seismic loads. However, the Northridge and Kobe earthquakes in 1994 and 1995, respectively, revealed that brittle failures occur widely at welded beam-to-column connections where traditional fully welded configurations promote large strain demands at critical points such as weld access holes [1]. Despite not causing structural collapse, these failures have thus highlighted fundamental gaps in the current understanding of steel structures' behaviours when subjected to seismic loading [2].

As a result of the 1994 Northridge earthquake, 150 steel structures failed due to brittle failure in beam-to-column connections. Such damage to connections was discovered in a wide range of buildings, both old to new and of all sizes. Initially, it was believed that these failures were due to poor workmanship; however, research initiated under the supplemental access control (SAC) protocol revealed a fundamental misunderstanding of the behaviours of welded moment connections during seismic loading. Such connections were thereby discovered to be incapable of dissipating energy effectively without causing significant damage to the building [3].

An extensive investigation was then undertaken by the SAC committee, which led to the publication of FEMA 350 [4]. During high-ductility demand, the two critical factors for failure are the tensions on the welded areas of the flange and web, and the connections. A common solution to this problem is to reduce ductility demands and related concentrations of tensions in these areas, and there have been several proposals for moment frame connections [4–7] to reduce the load on beam-column joints, many of which are sufficiently ductile in testing.

The reduced beam section (RBS) configuration is one of these in which the portions of the beam flange closest to the beam-to-column connection are removed. An RBS can also be viewed as a plastic hinge that occurs away from the joint, resulting in much of the ductility demand on such beams arising in the plastic hinge rather than the welded beam-to-column interface. There have been

numerous experimental [8–10] and analytical [11–13] studies demonstrating the efficacy of this solution, and according to experimental results [14], polyline-shaped solutions have the lowest rotational capacity with curved RBS.

In terms of the location and reduction rate of RBSs, FEMA 350 [4] and FEMA 351 [15] recommend certain design parameters based on the performances of tested beam-column connections. The European Commission has also presented recommended designs of such types of connections in its EC8, Part 3 [16] in the vein of previous recommendations. Table 1 presents the proposals for flange cut radius from FEMA 350, AISC 358-05 [17], and EC8, Part 3.

By optimising RBS cuts, the maximum plastic strain can be reduced to maximise the capacity for energy dissipation in the connection and reduce the fracture odds still further. Compared with the re-entrant angles seen on tapered or constant cuts, a review of tests conducted before 2000 [18] determined that radius cuts minimise stress concentration. Most studies conducted to date on cut-out optimisation have used pre-determined shapes [19]; however, a study by Pan et al. [20] examined the optimum shape for flanges under monotonic loads. The consideration of cyclic loads is, however, necessary for the seismic design.

The current paper thus presents numerical modelling results using the finite element analysis (FEA) implemented in ABAQUS [21] to validate the results for six sub-assemblies connected by RBS moments. This has several objectives: (1) to compare the ductility of all types of RBS connections; (2) to determine the effect of different types of RBS connections on the Von-Mises stress and equivalent plastic strain (PEEQ) at integration points in different zones; (3) to determine the effects of different forms of reduced flange sections on energy dissipation by the whole system; and (4) to examine exterior models for buckling behaviours.

Table 1: Geometrical properties of RBS

FEMA350-2000 ordinary moment frame, SMF [4]	EC8, Part 3 [16]	AISC 358-05 (IMF, SMF)
$a = (0.5 \text{ to } 0.75)b$ $b = (0.65 \text{ to } 0.85) d_b$ $c \le 0.25b$ $s = a + b/2$ $r = (4 c^2 + b^2)/8 c$	a = 0.6 b, $b = 0.75 d_b$ g = c : S 0.25b, s = a + b/2 $r = (4g^2 + b^2)/8g$	a = (0.5 to 0.75)b $b = (0.65 \text{ to } 0.85) d_b$ $0.l b_b \le c \le 0.25b$ —

2 Research methodology

For this analysis, the finite element method (FEM) was implemented in ABAQUS to obtain a more accurate and efficient solution. A numerical study was carried out on an exterior joint (T-shaped) model, which was considered an assemblage for this connection study.

Six RBS connections were thus modelled and analysed using ABAQUS, with the two samples tested experimentally by Pachoumis et al. [22] used to validate the ABAQUS results. After validation, four flange-cut geometry schemes were analysed: rectangular, trapezoidal, triangular, and drilled hole.

2.1 Design of specimens

The overall test setup and specimen geometry used by Pachoumis et al. [22] are shown in Figure 1. They investigated two specimens, designated as RBSa and RBSb, using an HE 300B column and HE 180 A beam for each sample. The authors used these sections with double web plates and continuity plates to produce a strong panel zone, equal in thickness to the beam's flange thickness, at each column. In this way, the plastic hinge was formed in the weakening zone. Three-point bending coupon tests were then used to determine the material properties of the beams, and the following values were obtained: elasticity modulus E = 209,000 MPa, yield stress fy = 310 MPa, and ultimate stress fu = 430 MPa [22].

The material properties of the weld were also considered. The other four specimens in this work are considered to have the same properties for the beam and column, with the only difference being the flange-cut pattern. Figure 2 shows the dimensions and flange-cut profiles for all specimens analysed in the current study.

2.2 FEA

In this study, the non-linear FE program ABAQUS [21] was adopted to investigate the response of RBS connections with various flange-cut patterns subjected to cyclic loading. HE 300B was used as a column and HE 180 A as a beam, as shown in the study by Pachoumis et al. [22]. All components of the typical RBS connections were

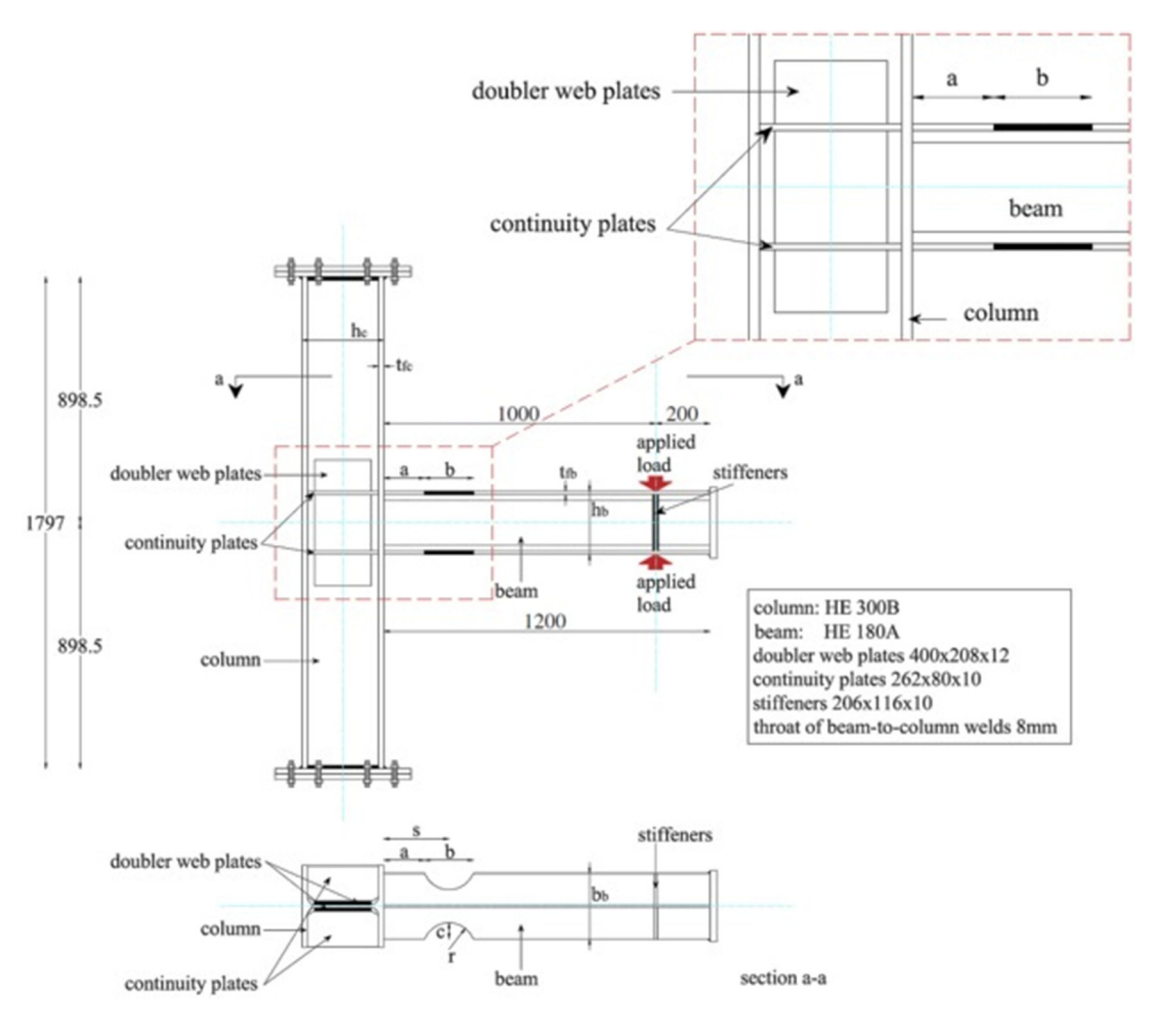


Figure 1: Specimen installation [22].

modelled using ABAQUS's thin shell elements (S4R). Due to the symmetry of the models, only half of each specimen was modelled to reduce run time, as shown in Figure 3. The material properties were defined by their bilinear elastic–plastic strain–stress relationships. The materials used for columns, beams, continuity plates, doubler plates, and stiffeners follow the curves shown in Figure 4.

2.3 Loading conditions

From the face of the column and at a distance of 1,000 mm, cyclic variable amplitude displacement was applied at the top of the beam. Following the AISC Seismic Provisions (AISC 2002) [24], the cyclic displacement amplitude followed a specific loading protocol. The loading protocol that

is shown in Figure 5 and Table 2 is used in ABAQUS. Here, δ_y represents the first yield deformation obtained from the static analysis of the model.

3 Results

3.1 Test verification

In this study, the FEM of RBS connections tested by Pachoumis et al. [22] has been used to verify the accuracy and applicability of a non-linear FEM. The properties and installation-tested specimens are shown in Figure 1. Figures 6 and 7 show the comparison of hysteretic curves of the current numerical results with the experimental results that are presented in ref. [22] for the two F specimens

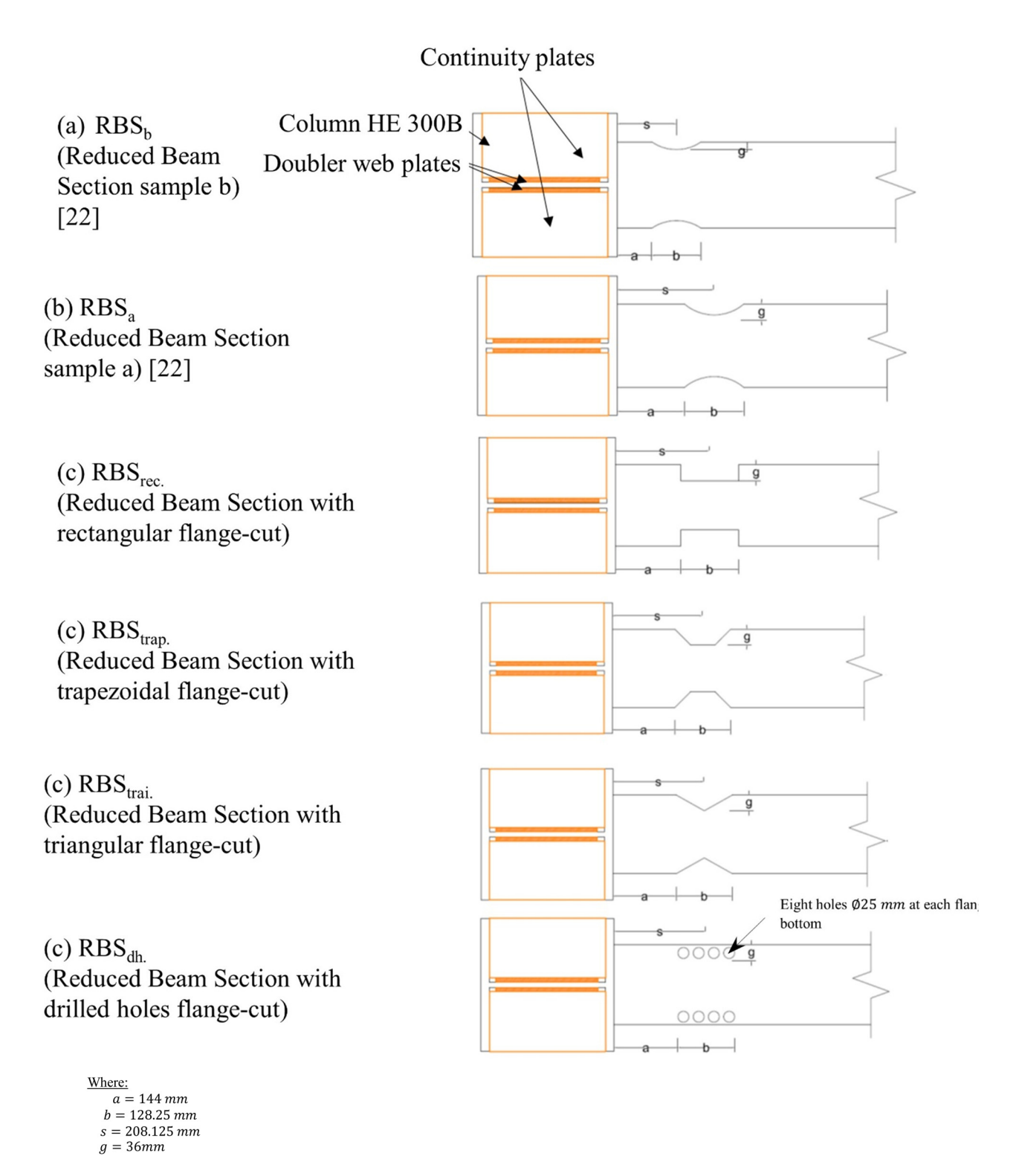


Figure 2: Dimensions and flange-cut profiles of all specimens tested in the present study.

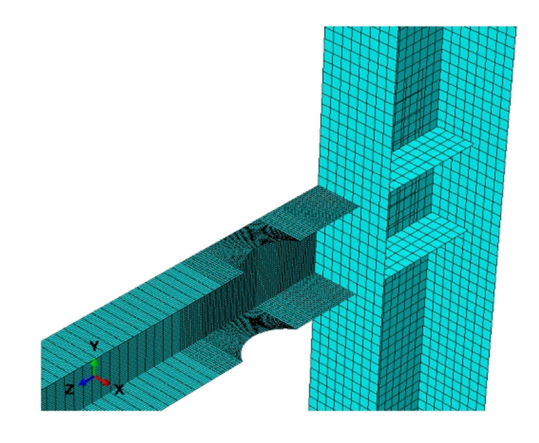


Figure 3: Finite element mesh of the RBS connection (element S4R).

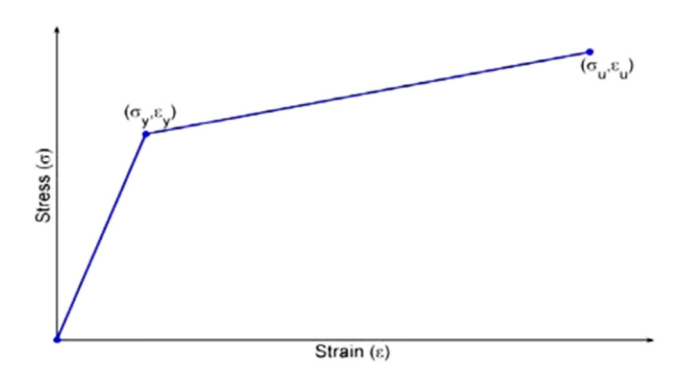


Figure 4: The elastic-plastic stress-strain model used in the present study.

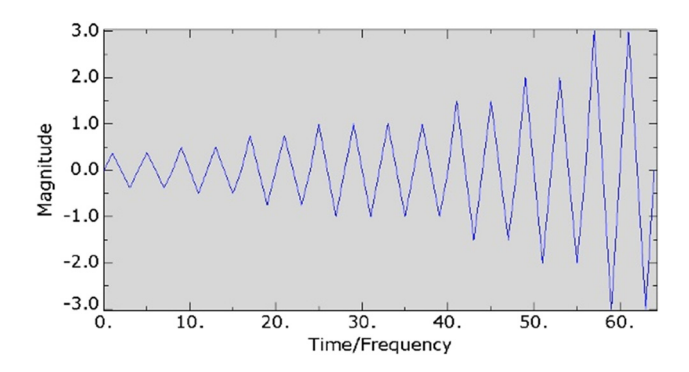


Figure 5: Loading protocol.

RBSa and RBSb, which indicates a good agreement between them. Therefore, the FEMs used in this study have a low error rate (a little over 6%).

Table 2: Loading protocol

Load step	Peak deformation, δy	Number of cycles, n
1	0.375	2
2	0.50	2
3	0.75	2
4	1.00	4
5	1.50	2
6	2.00	2
7	3.00	2

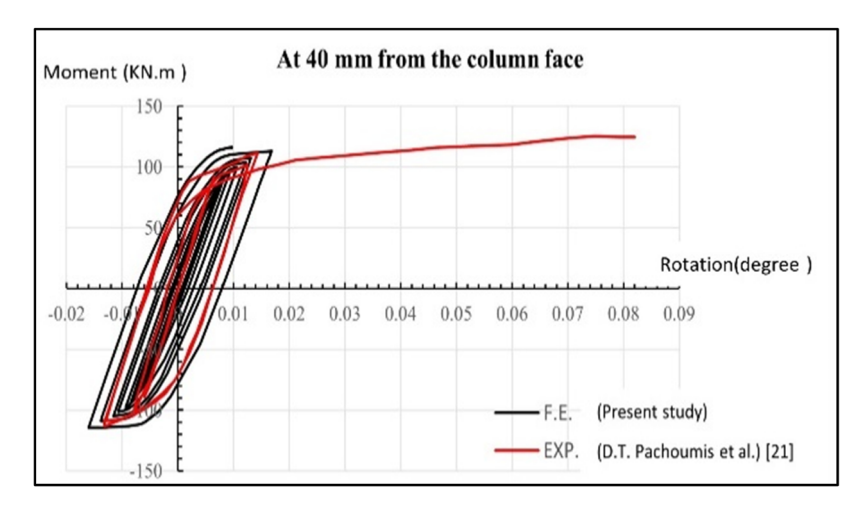
3.2 PEEQ and Von-Mises stress distribution

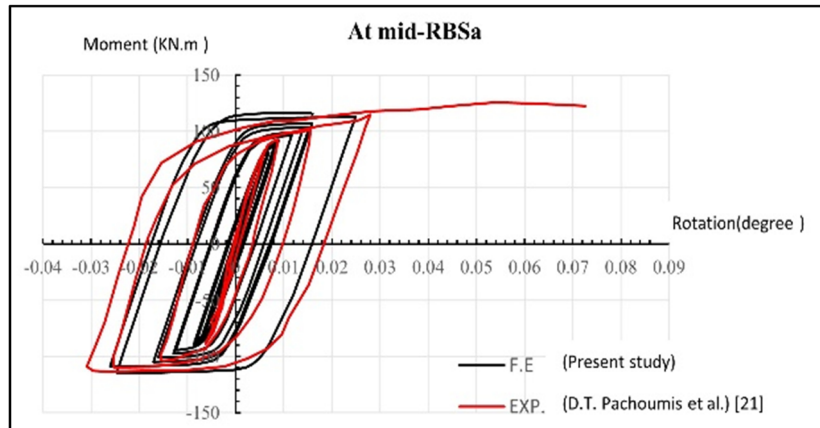
As illustrated in Figures 8 and 9, it was possible to calculate the PEEQ and Von Mises stress distributions for each specimen. An inelastic strain demand index (PEEQ) was used to measure the equivalent plastic-to-yield strain ratio.

Comparing the RBSa with the other specimens, the analytical results show that it has a uniform Von-Mises stress distribution and a lower PEEQ value (0.685), indicating that it has a higher degree of ductility. The PEEQ index for specimen RBSrec was 46% higher compared to that of RBSa, and there was 60.5% increase for specimen RBStrap compared to RBSa, while those for RBStri and RBSdh were 65.5 and 105.5%, respectively. RBSa thus has a greater potential for better plastic hinge formation away from the connection area, leading to better behaviours of RBSa connections in comparison to other connections. In addition, for both RBSrect (rectangular cut-flange profile) and RBStrap (trapezoidal cut-flange profile) specimens, the concentration of stress at the corners of the entrance led to a fracture of the beam flange at the narrowest section, while the specimen with drilled holes (RBSdh) showed clearly visible PEEQ concentration zones at the beam flanges, as shown in Figure 8.

3.3 Hysteretic curves and rupture index

A hysteretic curve for the moment-rotations resulting from the FE analysis is shown in Figure 10 for the midpoint of the RBS connections for the RBSrec, RBStrap, RBStri, and REBdh specimens. The results showed no local buckling in the beam web or flange of all specimens, and hence, no strength reduction was observed for any





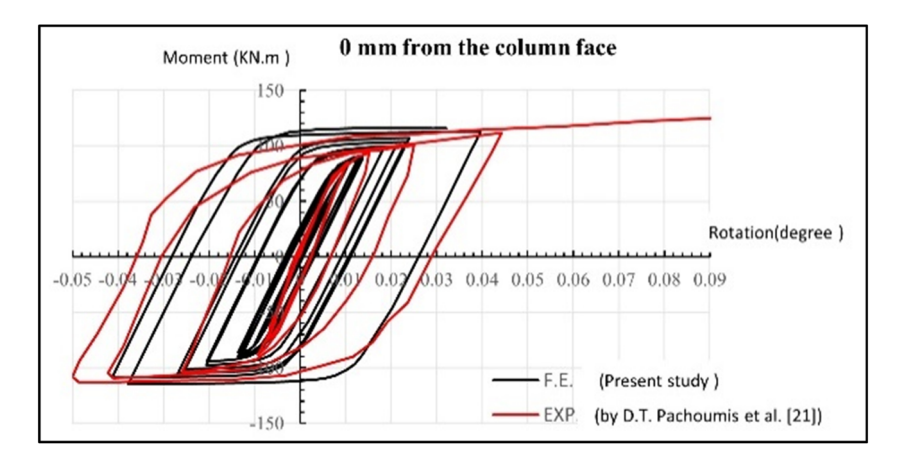
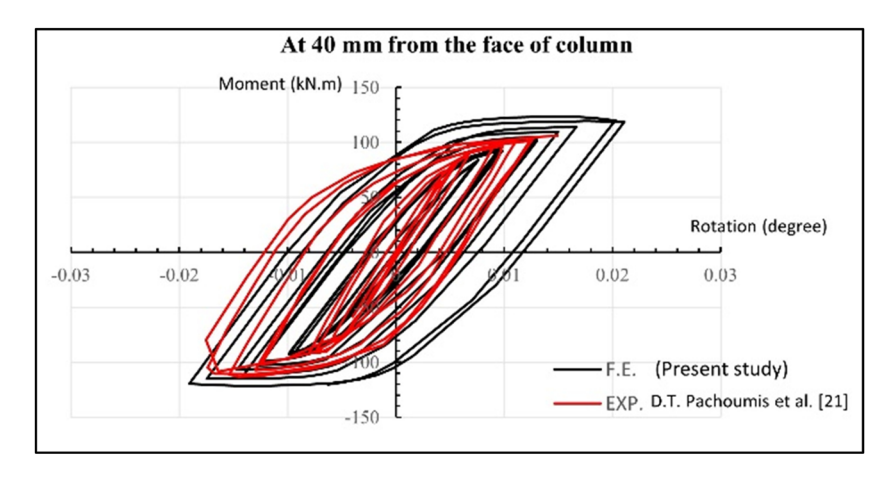
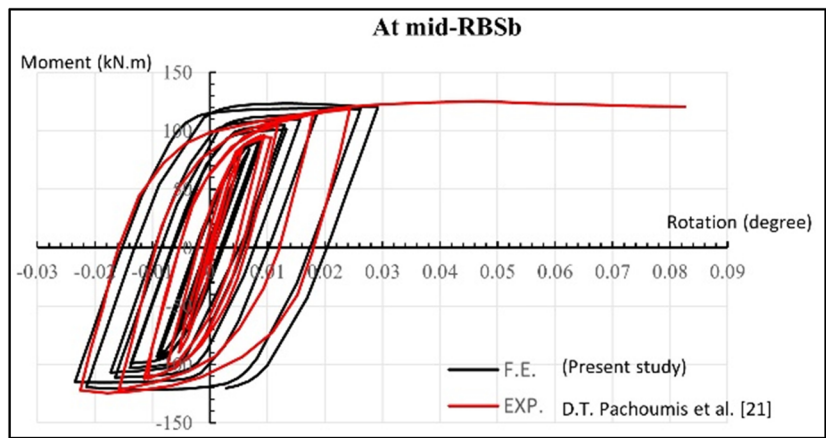


Figure 6: Comparison of numerical and experimental results of RBSa.

specimen except the RBStri connection, where local buckling was noted in the beam flange at 0.02 rad, causing this connection to be weakened by buckling on the web and flange.

The numerical analysis results allowed the rupture index (RI) to be calculated to assess the effects of various parameters on the ductile fracture potential of models with different cut-flange configurations. RI refers to the





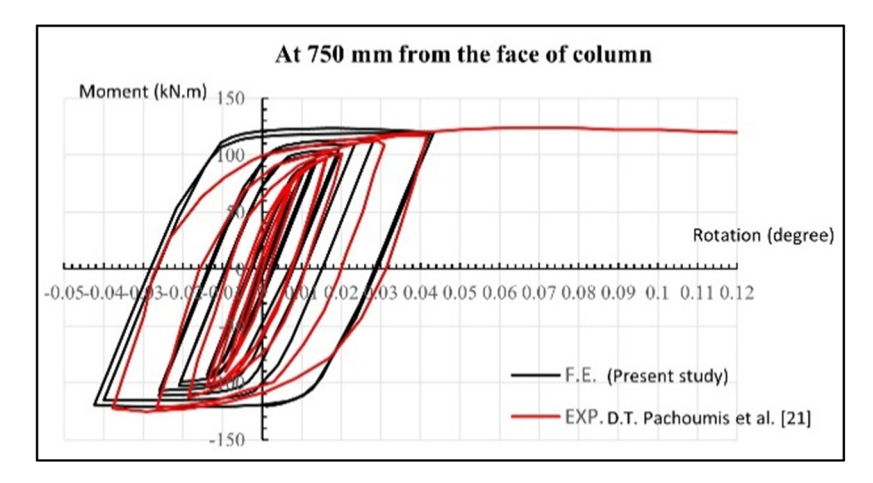


Figure 7: Comparison of numerical and experimental results of RBSb.

ratio between the PEEQ index and the ductile fracture strain, ϵ_f multiplied by the constant of material:

where q = Von-Mises stress and p = hydrostatic pressure, such that

$$RI = \alpha \cdot \frac{PEEQ/\varepsilon_y}{\varepsilon_f} = \frac{PEEQ/\varepsilon_y}{\exp\left(1.5\frac{p}{q}\right)}, \qquad (1) \qquad p = -\frac{1}{3} \times \operatorname{trace}(\sigma_{ij}) = -\frac{1}{3} \times \sigma_{ij}, \qquad (2)$$

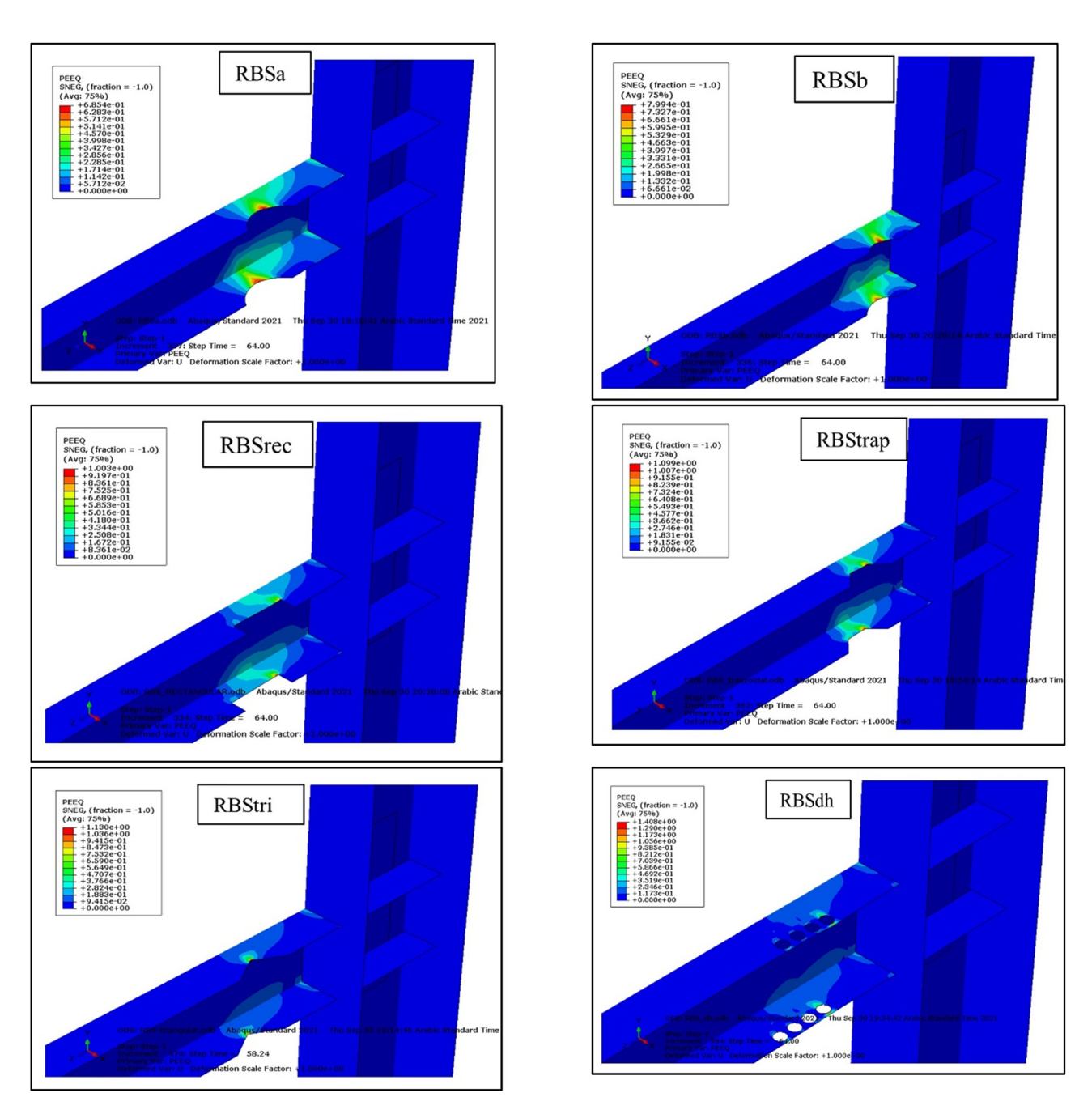


Figure 8: PEEQ distributions on the last cycle (3 \times $\delta_{y})$ for all specimens.

and

$$q = \sqrt{\frac{3}{2} S_{ij} S_{ij}}. ag{3}$$

The PEEQ is thus,

$$PEEQ = \sqrt{\frac{2}{3} \varepsilon_{ij}^{pl} \varepsilon_{ij}^{pl}}.$$
 (4)

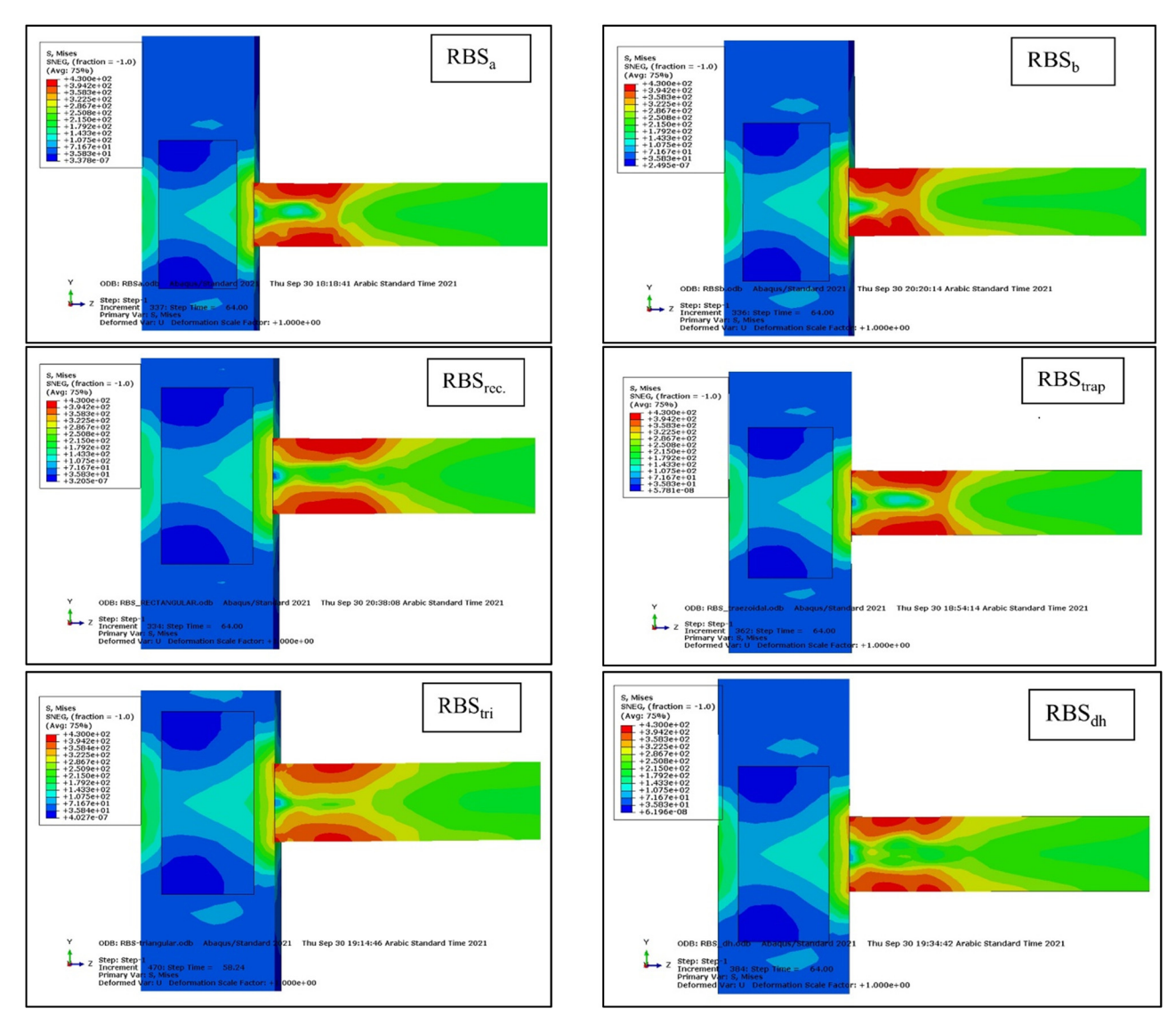


Figure 9: Von-Mises stress distributions on the last cycle $(3 \times \delta_{y})$ for all specimens.

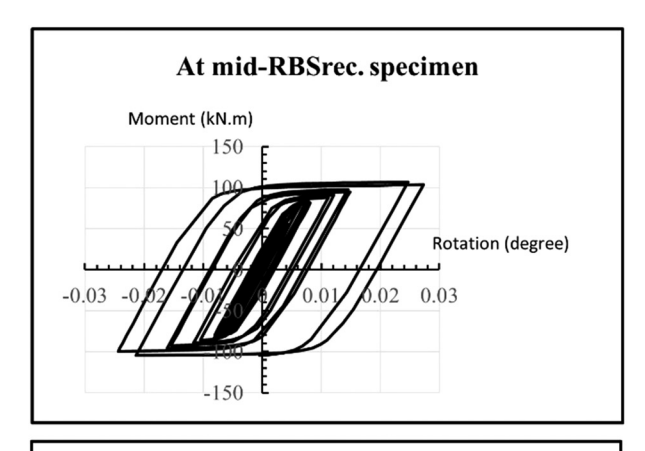
Based on FEA, Figure 11 shows the maximum values of RI for all tested specimens. These were developed to assess and compare the possibility of ductile fracture in finite element models at different places and between two distinct models at the same location. Hancock and MacKenzie [23] suggested that this criterion for determining the likelihood of a ductile fracture is accurate, and the RBS connection (RBSa) has a lower RI than the other specimens, as shown in Figure 11. The greater plastic stresses that form in the connecting zone along the column face are the source of the higher RI value in other specimens; however, in comparison to RBStrap, RBStri,

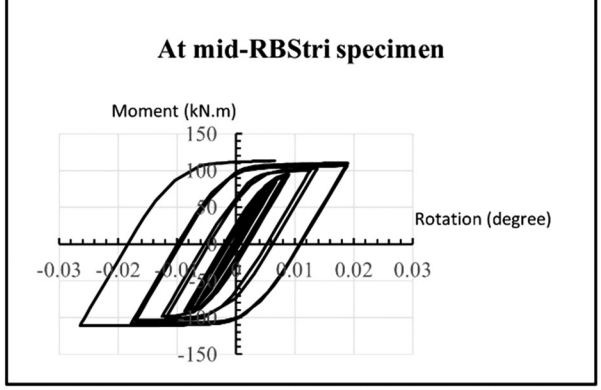
and RBSdh, RBSrec has a lower minimum value of RI, as shown in Figure 11.

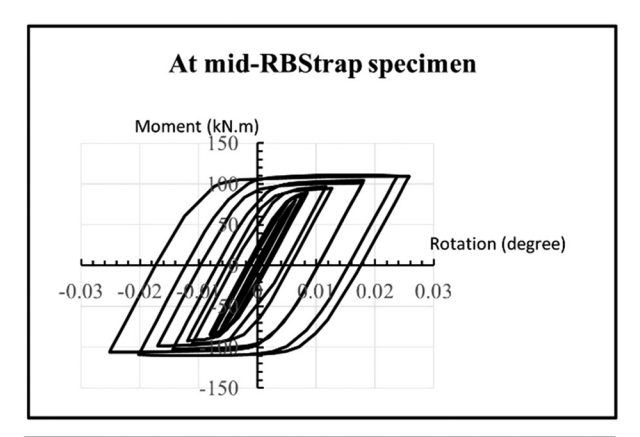
4 Conclusions

Based on the results of modelling using ABAQUS, the following conclusions were drawn:

1. For all connections, the maximum Von Mises stress intensity was 310–430 MPa at $3 \times \delta_y$ step loading. Stress intensities in the panel zone for all connections







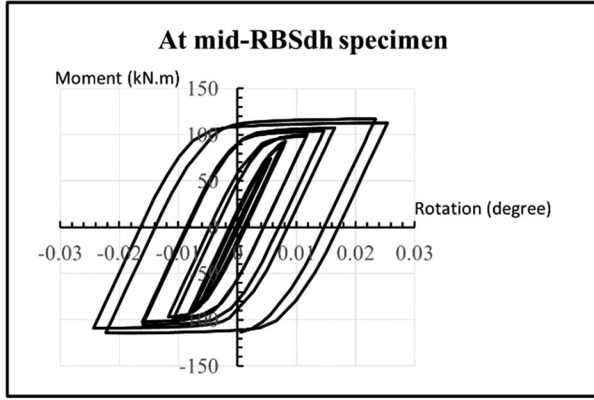


Figure 10: Cyclic moment-rotation and curves for tested specimens.

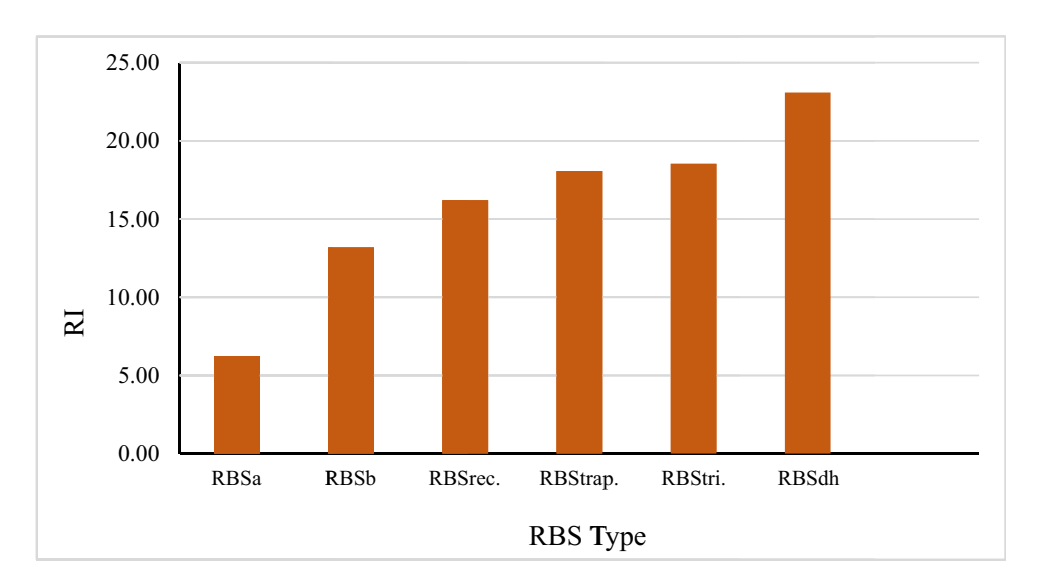


Figure 11: Effect of cut-flange type on RI.

- were between 150 and 250 MPa, with no yielding in the column.
- 2. The rectangular cut-flange profile offers greater ductility and energy dissipation than the trapezoidal, triangular, and drilled hole profiles.
- 3. The RBS connection with a circular cut-flange profile offers a lower RI than other connections.
- 4. Radius cut RBS have uniform stress contours. Any reentrant corner at the rectangular, trapezoidal, or triangular cut-flange profile connection may result in

- stress concentrations, however, leading to fracture of the flange.
- 5. The RI value was maximised in the RBS with drilled holes (RBSdh), which is thus less ductile than other tested connections in this study.

Conflict of interest: Authors state no conflict of interest.

References

- [1] Brunesi E, Nascimbene R, Rassati GA. Seismic response of MRFs with partially-restrained bolted beam-to-column connections through FE analyses. J Constr Steel Res. 2015;107:37–49. doi: 10.1016/j.jcsr.2014.12.022.
- [2] Gioncu V, Mazzolani F. Seismic design of steel structures.1st Edition. London: CRC Press; 2013.
- [3] Mahin SA. Lessons from damage to steel buildings during the Northridge earthquake. Eng Struct. 1998;20(4-6):261-70. doi: 10.1016/S0141-0296(97)00032-1.
- [4] FEMA 350, Recommended Seismic Design Criteria for New Steel Moment-Frame Buildings (FEMA 350), Washingt. (DC); 2000.
- [5] Engelhardt MD, Husain AS. Cyclic-loading performance of welded flange- bolted web connections. J Struct Eng. 1994;119(12):3537-50.
- [6] Tsai KC, Wu S, Popov EP. Experimental performance of seismic steel beam-column moment joints. J Struct Eng. 1995;925-31.
- [7] Plumier A. Behaviour of connections. J Constr Steel Res. 1994;29(1-3):95-119. doi: 10.1016/0143-974X(94)90058-2.
- [8] Engelhardt MD. The 1999 T. R. Higgins lecture: design of reduced beam section moment connections. 1999 North Am. Steel Constr. Conf; 1999. p. 1999.
- [9] Chen SJ, Chu JM, Chou ZL. Dynamic behaviour of steel frames with beam flanges shaved around connection. J Constr Steel Res. 1997;42(1):49-70. doi: 10.1016/S0143-974X(97) 00011-4.
- [10] Popov E, Blondet M, Stepanov L Application of dog bones for improvement of seismic behaviour of steel connections. Report no UCB/EERC 96/05. USA; 1996.

- [11] Anastasiadis A, Gioncu V. Influence of joint details on the local ductility ofsteel moment resisting frames. Proceedings of 3rd national Greek conference on steel structures; 1998. p. 311–19.
- [12] Anastasiadis A, Gioncu V, Mazzolani FM. New upgrading procedures to improve the ductility of steel MR-frames. XVII CTA Congress; 1999. p. 193–204.
- [13] Faggiano B, Landolfo R. Seismic analysis of steel MR frames with dog bone connections. Proceedings of 12th European conference on earthquake engineering; 2002. p. 309.
- [14] Engelhardt MD, Sabol TA. Seismic-resistant steel moment connections: developments since the 1994 Northridge earthquake. J Prog Struct Eng Mater. 1997;1(1):68-77.
- [15] FEMA 351. Recommended seismic evaluation and upgrade criteria for existing welded steel moment frame buildings. Washington (DC); 2000.
- [16] EC 8. Part 3: design of structures for earthquake resistance. Assessment and retrofitting of buildings. EN 1998-3; June 2005.
- [17] ANSI, A. AISC 358-05. Prequalified connections for special and intermediate steel moment frames for seismic applications. American Institute of Steel Construction Inc., Chicago; 2005.
- [18] Engelhardt MD, Fray GT, Venti M, Jones S, Holliday S. behaviour and design of radius cut, reduced beam section connections. Technical report. Sacramento (CA): SAC Joint Venture; 2000.
- [19] Jones SL, Fry GT, Engelhardt MD. Experimental evaluation of cyclically loaded reduced beam section moment connections. J Struct Eng. 2002;128(4):441-51.
- [20] Pan P, Ohsaki M, Tagawa H. Shape optimization of H-beam flange for maximum plastic energy dissipation. J Struct Eng ASCE. 2007;133(8):1176-9.
- [21] ABAQUS/PRE, Users Manual, Hibbit, Karlsson and Sorensen Inc.; 1997.
- [22] Pachoumis DT, Galousis EG, Kalfas CN, Efthimiou IZ. Cyclic performance of steel moment-resisting connections-experimental analysis and finite element model simulation, J. Eng Struct. 2010;32:2683-92.
- [23] Hancock JW, MacKenzie AC. On the mechanisms of ductile failure in high-strength steels subjected to multi-axial stressstates. J Mech Phys Solids. 1976;24:147-69.
- [24] American Institute of Steel Construction AISC. Seismic provisions for structural steel buildings. Chicago; 2002.